

Asymmetric Fullerene Nanosurfactant: Interface Engineering for Automatic Molecular Alignments

Dae-Yoon Kim, Sang-A Lee, Soeun Kim, Changwoon Nah, Seung Hee Lee, and Kwang-Un Jeong*

Since the molecular self-assembly of nanomaterials is sensitive to their surface properties, the molecular packing structure on the surface is essential to build the desired chemical and physical properties of nanomaterials. Here, a new nanosurfactant is proposed for the automatic construction of macroscopic surface alignment layer for liquid crystal (LC) molecules. An asymmetric nanosurfactant ($C_{60}NS$) consisted of mesogenic cyanobiphenyl moieties with flexible alkyl chains and a [60]fullerene nanoatom is newly designed and precisely synthesized. The $C_{60}NS$ directly introduced in the anisotropic LC medium is self-assembled into the monolayered protrusions on the surface because of its amphiphilic nature originated by asymmetrically programmed structural motif of LC-favoring moieties and LC-repelling groups. The monolayered protrusions constructed by the phase-separation and self-assembly of asymmetric $C_{60}NS$ nanosurfactant in the anisotropic LC media amplify and transfer the molecular orientational order from surface to bulk, and finally create the automatic vertical molecular alignment on the macroscopic length scale. The asymmetric $C_{60}NS$ nanosurfactant and its self-assembly described herein can offer the direct guideline of interface engineering for the automatic molecular alignments.

1. Introduction

Precise control over structural motifs and their macroscopic molecular ordering on different length scales is a central research topic in the fields of materials science and engineering, promoting the creation of novel functional materials for high performance devices.^[1,2] In this aspect, the manipulation of molecular arrangements in liquid crystal (LC) mesophases attracts much interest, since the intrinsic fluidity and structural anisotropy of LC result in facile responses to interfacial and


external forces, rendering these molecules useful for applications in photonic displays and biological sensors.^[3,4] Since advanced LC technology requires the uniform molecular orientations either homogeneous or homeotropic, the development of novel alignment layers has been attempted.^[5,6] From a fundamental perspective, molecular orientations are created by the chemical and physical interactions between substrate and LC known as surface anchoring, with evaporated oxides, patterned monolayers, photobuffed films, and mechanically rubbed polymers widely used as surface modifying materials for fulfilling this purpose.^[7,8]

Recently, nanoscience and nanotechnology have achieved fascinating breakthroughs in molecular orientations, enabling the formation of vertical alignment (VA) or planar alignment (PA) by introducing minute amounts of nanoparticles into the host LC medium.^[9] These nanoparticles are gradually diffused and

deposited on the substrate, which is a thermodynamically more stable state.^[10] The modified surface by self-assembled nanoparticles can induce the alignment of LC molecules in defined directions without any additional pretreatment.^[11] Dispersions of gold spheres, nickel bowls, and carbon nanotubes are good examples of agents achieving the uniform LC alignments by optimizing their shape, size, and concentration, resulting in this exciting invention being geared toward the one-bottle approach.^[12] In addition, the use of nanoparticles in LC media has improved the electro-optical performances, achieving high contrast ratios, fast response times, and low driving voltages.^[13] Therefore, many organic chemists and device physicists have focused on the nanoparticle-induced automatic LC alignment for the technologically significant nanoscale manufacturing.^[14] Although LC orientation achieved by the simple addition of nanoparticles is a facile and economically viable process, it exhibits several reliability issues.^[15] Since interactions between individual nanoparticles are stronger than those between nanoparticles and LC molecules, the former often form the macroscopic aggregates that cause severe light scatterings.^[16]

To overcome the notorious aggregation of nanoparticles in the anisotropic LC media, various methods for achieving automatic LC alignment have been developed, including functionalized nanoparticles referred to as organic-inorganic hybrid

D.-Y. Kim, S.-A. Lee, S. Kim, Prof. C. Nah, Prof. K.-U. Jeong
BK21 Plus Haptic Polymer Composite Research Team & Department
of Polymer-Nano Science and Technology
Chonbuk National University
Jeonju 54896, South Korea
E-mail: kujeong@jbnu.ac.kr
Prof. S. H. Lee
Department of BIN Convergence Technology
Chonbuk National University
Jeonju 54896, South Korea

 The ORCID identification number(s) for the author(s) of this article can be found under <https://doi.org/10.1002/smll.201702439>.

DOI: 10.1002/smll.201702439

materials.^[17,18] The enhancement of intermolecular interactions between nanoparticles and LC molecules achieved by chemical modification does not necessarily result in the materials with maximally improved physical properties, since functional groups on the nanoparticle surface are randomly distributed.^[19,20] Thus, materials with poorly defined structures and morphologies can limit the formation of uniform LC alignment.^[21] To keep pace with the rapid changes in the ever-growing sophistication of molecular design, chemical functions should be introduced into nanoparticles in a programmed manner.^[22,23] We expect the utilization of site-selective functionalized nanoparticles to be helpful for predicting the collective interaction of surface functions of LC media and solid substrates to achieve the automatic molecular alignment. An example of this strategy is the utilization of nanoparticles with a well-defined molecular structure and specific symmetry, e.g., fullerenes, polyhedral oligomeric silsesquioxanes, and polyoxometalates.^[24,25] Among them, [60]fullerene (C_{60}) is an intriguing nanoparticle, being small, stable, and readily available with its stoichiometry-controlled Bingel–Hirsch and Retro-Prato reactions allowing the preparation of monoadducts.^[26,27]

In view of the above, we proposed an amphiphilic and asymmetric nanosurfactant bearing LC-favoring organic functions directly tethered to LC-repelling nanoparticles, with its C_{60} head group specifically modified to induce 2D monolayer formation on solid substrates. The above modification was performed by attaching cyanobiphenyl mesogens and alkyl chains to the nanobuilding block of C_{60} , resulting in an asymmetric nanosurfactant (abbreviated as $C_{60}NS$) capable of bridging the solid substrates and LC molecules. Initially, we examined the automatic VA of LC molecules induced by the direct introduction of $C_{60}NS$ nanosurfactants and systematically investigated its self-organization in the host LC media. The observed electro-optical switching of an LC test cell confirmed that the proposed technology allows the fabrication of cost effective optoelectronic devices for large area platforms.

2. Results and Discussion

The asymmetric $C_{60}NS$ nanosurfactant designed and synthesized for the automatic molecular alignment could be used to fabricate electrically controllable birefringence modulators. The $C_{60}NS$ was synthesized by utilizing the Bingel reaction to covalently connect the rod-like twin cyanobiphenyl derivative (BP_2T) to the periphery of the C_{60} nanoparticle with flexible alkyl chain spacers (**Figure 1**).^[28] Detailed synthetic procedures and analytical data for $C_{60}NS$ and related intermediates, such as nuclear magnetic resonance (NMR), elemental mass (EM), ultraviolet-visible (UV-vis), and Fourier transform infrared (FT IR) spectra, can be found in Figures S1–S7 in the Supporting Information. The chemical structures and physical properties of $C_{60}NS$ indicate that its phase-separation from the

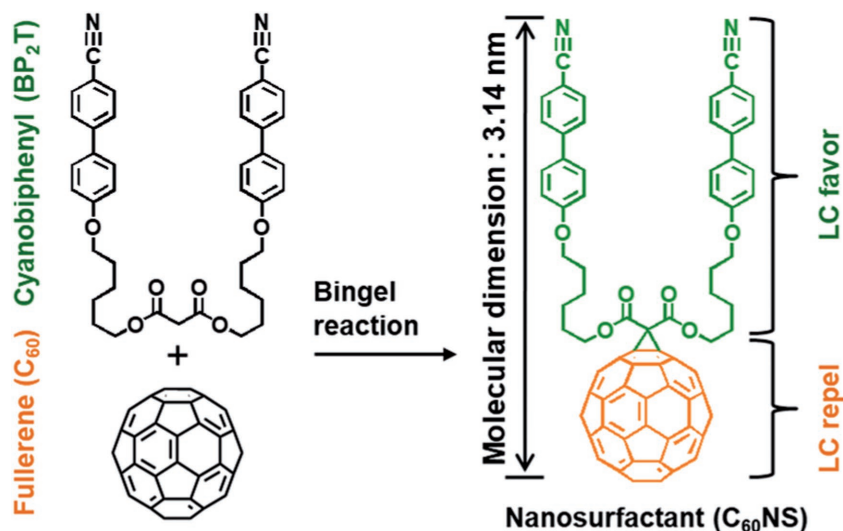


Figure 1. Synthetic procedure of asymmetric $C_{60}NS$ nanosurfactant by the Bingel reaction.

host LC medium and the subsequent self-assembly on the solid substrates can automatically influence the surface anchoring conditions for molecular orientation. As shown in **Figure 1**, the asymmetric $C_{60}NS$ nanosurfactant consists of two different segments: the incorporated BP_2T units determine interactions with anisotropic LC media, whereas the C_{60} core, exhibiting an inherent aggregation tendency, directly interacts with solid substrates to minimize surface energy.^[29]

To identify the key factors influencing the automatic alignments of molecules, interactions between anisotropic media, surfactant materials, and solid substrates were first studied by polarized optical microscopy (POM), with results shown in **Figure 2**. The homogeneous LC mixtures with BP_2T , C_{60} , and $C_{60}NS$ were prepared respectively and filled into an indium tin oxide (ITO)-coated LC cell sandwiched by 10 μm spacers. In the case of BP_2T and C_{60} within the LC medium, no automatic VA of LC was observed in the macroscopic region. Note that the Schlieren texture observed by POM was a typical characteristic of nematic phase in PA anchoring condition.^[30] PA of LC molecules on ITO-coated substrates was observed when the introduced materials represent two extreme cases, e.g., contain LC-favoring moiety of BP_2T and LC-repelling group of C_{60} . The LC medium fully dissolved the BP_2T due to the similarity of their chemical structure with that of host LC molecules. On the other hand, neat C_{60} nanoparticles were immediately precipitated from the host LC medium, forming numerous aggregates with the micrometer length scales. Additionally, in the case of other chemically modified C_{60} nanoparticles, such as methyl ester or carboxylic acid functions, also show only the PA arrangements of LC due to its self-segregation (**Figure S8**, Supporting Information). Therefore, one can safely conclude that BP_2T and C_{60} on their own cannot fulfill the condition of VA anchoring for LC molecules.

Surprisingly, the addition of $C_{60}NS$ nanosurfactant resulted in the automatic construction of a perfect VA layer of LC molecules. As shown in **Figure 2**, a complete dark state was detected by orthoscopic POM image when $C_{60}NS$ was doped into the LC cell at a loading of 0.1 wt%. The Maltese cross observed in

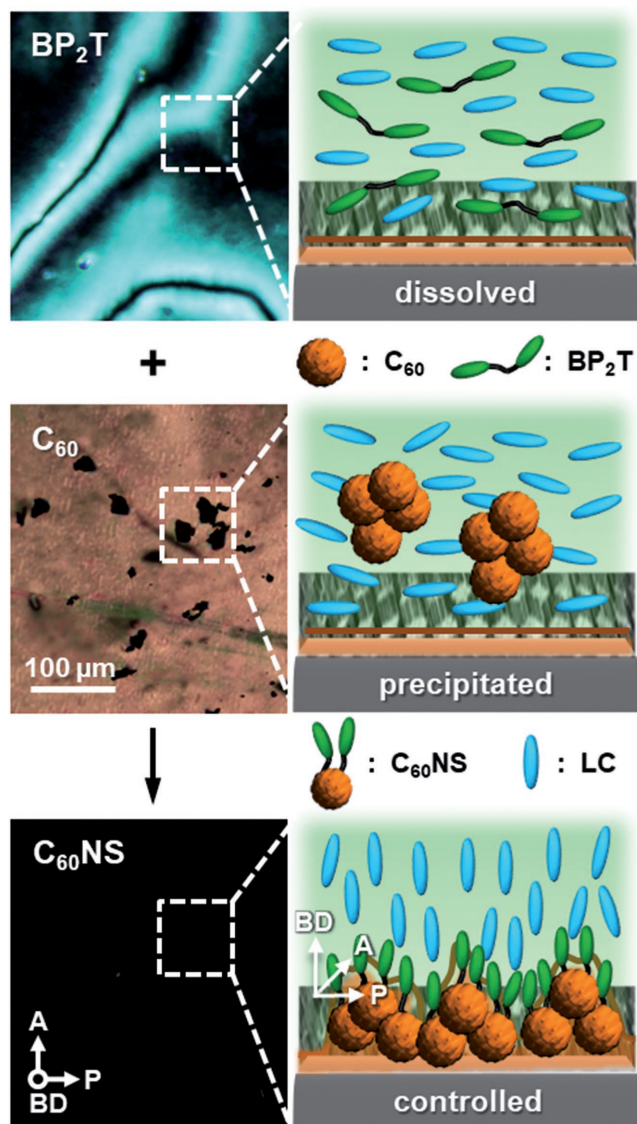


Figure 2. POM microphotographs and schematic illustrations of LC cells filled with 0.1 wt% BP₂T (top), C₆₀ (middle), and C₆₀NS (bottom). Analyzing (A), polarizing (P), and beam directions (BD) are additionally indicated.

the conoscopic POM image clearly indicates the homeotropic alignment of LC molecules (Figure S9, Supporting Information).^[31] The solubility of C₆₀NS in the LC medium was finely tuned by the combination of LC-favoring groups and LC-repelling building blocks. The BP₂T moieties of C₆₀NS increase its compatibility with host LC molecules and avoid macroscopic self-aggregation, whereas C₆₀ groups favor the gradual phase-separation of C₆₀NS from the LC medium and its subsequent migration onto solid substrates. We conjecture that the deposition of nanosurfactant on the surfaces is responsible for a VA of LC.

Here, the orientational director of the LC (n) could be visualized by a specifically designed experiment, utilizing a nematic diacrylate monomer, so-called reactive mesogen (RM), which could be polymerized by irradiating UV light.^[32] The schematic

presentation of experimental procedures for pathway 1 is depicted in Figure S10 in the Supporting Information. Briefly, optical cells were filled with LC mixtures containing 0.1 wt% of C₆₀NS and 2.0 wt% of RM. At the initial stage, all compounds were randomly oriented. After the above-mentioned phase-separation and self-organization of C₆₀NS, anisotropic molecules were oriented perpendicular to the substrate. The optical cell was then irradiated with UV light to initiate polymerization.^[33] The dark states observed in POM images indicate that anisotropic molecules exhibited the uniform VA before and after in situ photopolymerization (Figure S11, Supporting Information). A few minutes later, the photopolymerization was quenched, the unreacted RM and LC were removed using hexanes, and the optical cell was carefully opened. The n related to the adsorbed C₆₀NS on the substrate was ultimately confirmed by scanning electron microscopy (SEM). The polymer network is uniform, in accordance with the LC coverage of C₆₀NS layers. As shown in Figure S12 (Supporting Information), the cross-sectional image of the fractured optical cell along the film thickness direction exhibits the fibrous polymer network oriented perpendicular to the substrate. Note that the RM can be effectively oriented along n .^[34] Therefore, the VA of the host LC medium was successfully transferred to the polymer template during the in situ photopolymerization of RM. As a result, it is realized that the LC order driven by C₆₀NS nanosurfactant is indeed VA.

The birefringence controlled optics and organic replicating methods directly verified the VA of the LC by doping the C₆₀NS. Now, we have extensively studied the inner surface to undertake intensive research on the mechanism of automatic LC alignment induced by nanosurfactant. Since the automatic construction of VA layers is closely related to the controlled compatibility between C₆₀NS and host LC molecules as well as to the optimized concentration of C₆₀NS in the host LC medium, LC molecular alignment should be investigated as a function of the C₆₀NS concentration. Transmissive POM images were acquired for variable C₆₀NS contents in LC mixtures using the Bertrand lens, with results presented in Figure 3.^[35] As shown in Figure 3a, several micrometer sized particles were detected in the LC cell containing 1.0 wt% of C₆₀NS. There is no sign for the VA of LC. At high concentrations, the severe aggregation occurred via the coalescence of C₆₀NS, disturbing the construction of 2D uniform layers and resulting in the formation of 3D microparticles. Notably, multifold LC domains were randomly oriented.

The aggregation behavior of C₆₀NS could be inferred from its bulk molecular packing structure. Figure 4a shows X-ray diffraction (XRD) patterns of C₆₀NS obtained at room temperature. A sharp reflection peak at 3.66 nm was observed in the small-angle region, attributed to the (001) reflection of a lamellar structure.^[36] It is worthy to note that an average layer spacing (L) of ≈ 3.6 nm matches the periodic width of the lamellar structure directly observed in transmission electron microscopy (TEM) image.^[37] Thin films of C₆₀NS were prepared for TEM experiments via the drop casting method from the 0.1 wt% of C₆₀NS in chloroform solution. Bright-field TEM images of C₆₀NS films are shown in Figure 4b. Alternative dark and bright stripes are observed owing to the disparity in electron density of the fullerene-rich and the cyanobiphenyl-rich phase.^[38] The diffused

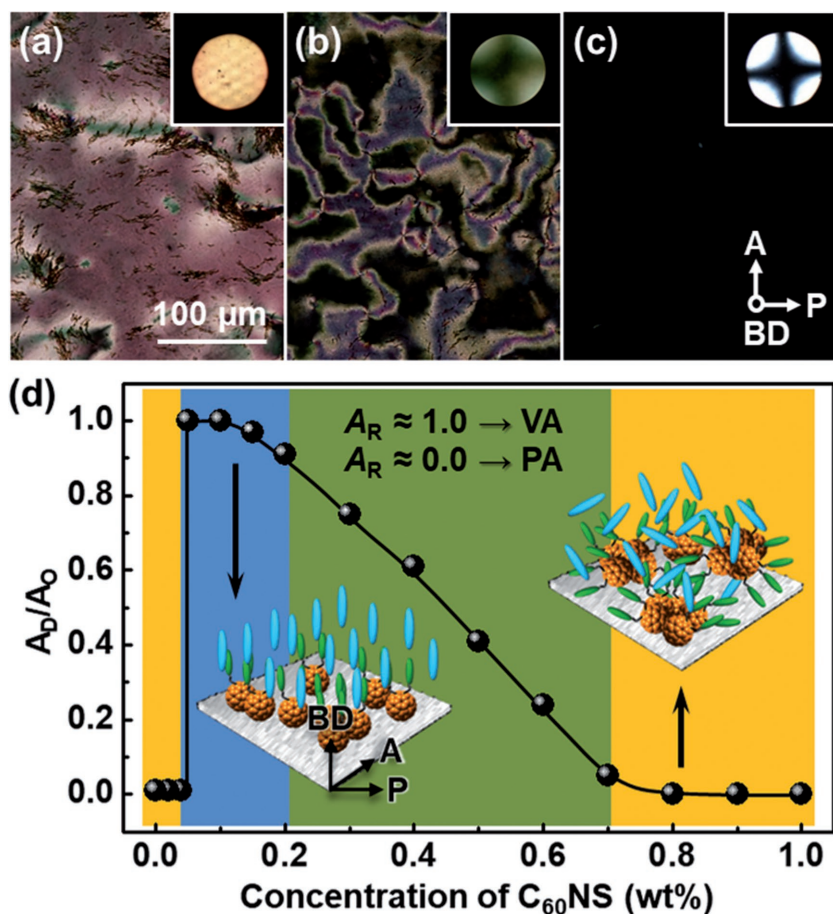


Figure 3. Orthoscopic and conoscopic (inset) POM images of LC cells containing a) 1.0, b) 0.5, and c) 0.1 wt% of C₆₀NS. d) Ratio of dark area (A_D) and total area (A_O) for different concentrations of C₆₀NS.

reflection at 0.92 nm was attributed to the interaction between partially ordered states of C₆₀ moieties, whereas the broad halo in the wide-angle region centered at 0.46 nm was ascribed to the lateral molecular packing of mesogenic groups.^[39] Based on the electron density fluctuations, neighboring layers were constructed by cyanobiphenyl mesogens aligned parallel to the layer normal direction, with flexible and hydrophobic alkyl chains located between neighboring layers.^[40]

The primary driving force for the self-assembly of C₆₀NS was the nanosegregation of structural motif.^[41] At high concentrations, the lamellar structure underwent agglomeration prior to experiencing phase-separation from the host LC medium.^[42] To alter the surface topography for the VA of LC, the content of C₆₀NS was deliberately reduced to prevent its self-aggregation. When C₆₀NS was introduced into the LC cell at a loading of 0.5 wt%, the dark region became broader, and a Maltese cross was observed (Figure 3b). It means that the VA of LC is locally achieved. Birefringent LC domains indicated that macroscopic aggregate of C₆₀NS were present, as opposed to its deposition on solid surfaces. However, it is worth noting that controlling the subtle balance of intermolecular interactions between the nanosurfactant and LC molecules exerts a deep influence on the phase-separation.

To understand the correlation between nanosurfactant concentration and LC orientation in detail, quantitative analyses were performed by calculating the ratio (A_R) of dark area (A_D) to the entire area (A_O).^[43] Figure 3d shows that A_R decreases with increasing C₆₀NS concentration, approaching zero at concentration above 0.7 wt% and confirming that the PA of LC is maintained, whereas A_R values between zero and unity indicates the coexistence of PA and VA. When the concentration of C₆₀NS was decreased to 0.1 wt%, the VA of LC was detected without any light scattering (Figure 3c), supported by the perfect dark state with a distinct Maltese cross pattern and maximum A_R. The detection limit for molecular alignment corresponded to 0.05 wt% of C₆₀NS in the LC mixture, since this nanosurfactant was totally dissolved in the host LC medium at lower concentrations. However, the transition from PA to VA indicated that controlled diffusion of C₆₀NS on the substrate resulted in the homeotropic LC anchoring.

The arising question is how the C₆₀NS nanosurfactants are put together into aggregates and deposited on the surfaces. To investigate this object, first, the homeotropically oriented sample was prepared via one-bottle approach using the LC mixture doped with 0.1 wt% of C₆₀NS. Then, the LC cell was immersed into hexanes to selectively remove LC molecules, followed by disassembly of the sandwiched cell using a scalpel and subsequent drying to evaporate residual solvents. Further analysis was performed using X-ray

photoelectron spectroscopy (XPS), which was a sensitive and quantitative method for probing the elemental composition of surfaces.^[44] Figure 5a shows an XPS survey scan, and deconvoluted XPS spectra of C₆₀NS film are shown in Figure 5b. The observed binding energies were assigned to aromatic C–C/C=C (284.5 eV), C≡N (298.8 eV) in cyanobiphenyl moieties, as well as C–O (285.7 eV) and C=O (288.1 eV) in ester linkages.^[45] The C1s, N1s, and O1s peaks correspond to the main constituents of C₆₀NS, implying that the phase-separated nanosurfactant is well deposited onto the substrate.

The morphology of the self-assembled C₆₀NS film on the substrate was also investigated by atomic force microscopy (AFM). Figure 5c shows that the use of 0.1 wt% C₆₀NS resulted in a surface exhibiting numerous protrusions with an average height profile of 3.02 nm.^[46] The surface of bare ITO-coated substrate was relatively smooth (Figure S13, Supporting Information). The root-mean-square roughness of the nanosized continuous layer is about 2.87 nm (Figure 5d). Since the calculated geometric length of C₆₀NS along the long axis was about 3.14 nm, this result indicated that nanosurfactant was assembled into monolayers, as additionally confirmed by water contact angle (WCA) measurements.^[47] The bare ITO-coated substrate showed a WCA of 79.4°, whereas that of C₆₀NS

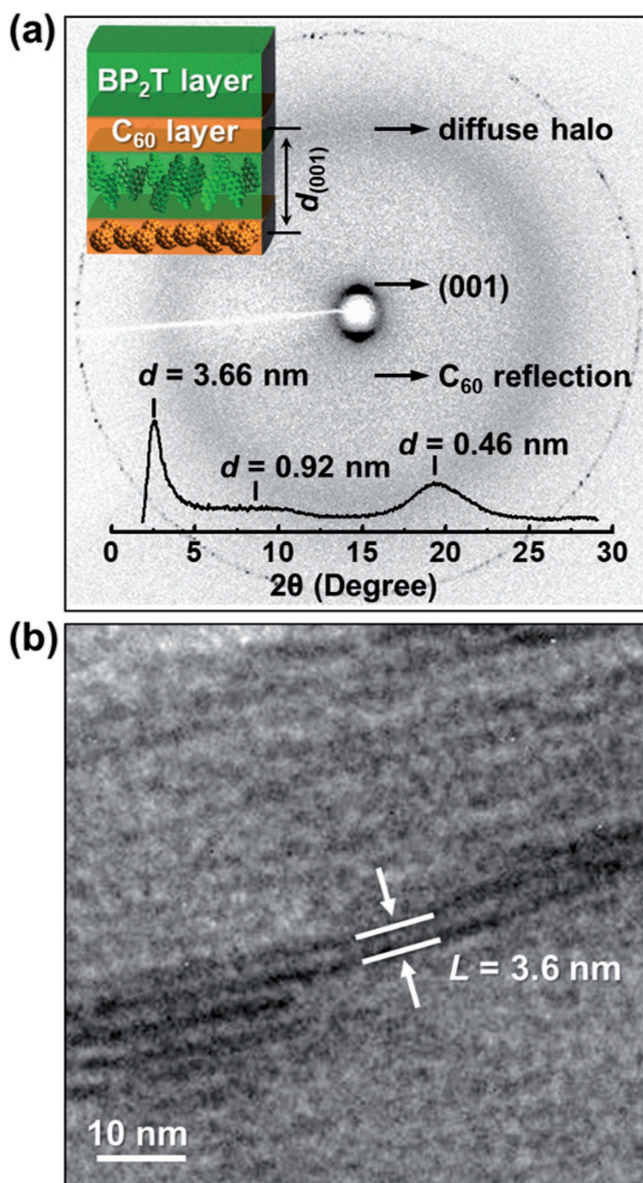


Figure 4. a) XRD pattern and b) TEM image of C_{60} NS bulk sample, and the schematic illustration of C_{60} NS arrangement (the inset of panel (a)).

film equaled 96.8° , suggesting the formation of a hydrophobic layer (Figure S14, Supporting Information). The line scans in Figure 5e revealed that C_{60} NS monolayer was 3.08 nm high and 979 nm wide. Based on the topographical features, the monolayered 2D protrusions were constructed by lateral close packing of C_{60} NS nanosurfactant on the solid substrate, with its molecular axis being parallel to the surface normal. From the results of optical, morphological, and spectroscopic analyses, the C_{60} NS-doped in the LC was observed clearly adsorbing on the inner surface of the substrates. In fact, the programmed nanosurfactant worked as the automatic alignment layers of the LC cells.

We motivate this study by identifying C_{60} NS nanosurfactant and LC mixtures as of potential interest in VA mode device, which is dominantly adapted for the application in the LC

display industries.^[48] To test the applicability of the above mixtures to fabricating such devices, we constructed a multidomain LC cell with a patterned pixel electrode (width = 3.0 μm , distance = 4.0 μm) on the bottom substrate and a nonpatterned common electrode on the top substrate, and filled it with an LC mixture containing 0.1 wt% of C_{60} NS (inset of Figure 6a). In voltage OFF state, the macroscopic image of the LC cell displayed a uniform dark state under crossed polarizers. Figure 6a shows precisely matching characteristics of the VA of LC. In order to confirm the electro-optical switching properties, the electrically controlled birefringence followed by n was determined from the voltage-dependent transmittance curve of the 0.1 wt% C_{60} NS-doped LC cell under crossed polarizers.^[49] Upon applying voltage, the orientation of LC was changed from VA to PA, accompanied by an increase of transmittance (Figure 6c). The bright state of LC textures with uniform transmittance was detected, indicating that LC molecules were rearranged to exhibit PA by the above electric (E) field (Figure 6b).^[50] The n in the voltage ON state was also visualized using the above-mentioned method. In this case, the in situ photopolymerization of LC mixtures containing 0.1 wt% of C_{60} NS and 2.0 wt% of RM was performed under an applied E field by following the pathway 2. The SEM image for fractured surface is shown in Figure S15 in the Supporting Information, showing that the fibrous anisotropic polymer network is aligned parallel to the substrate. Therefore, it was realized that n was tilted toward azimuthal plane of the substrate in the field ON state.

The formation of the monolayer film leads to the reasonable suggestion that C_{60} NS induces the automatic VA of LC. The C_{60} NS-doped in LCs would adsorb on the substrates to minimize the surface energy. Although the theoretical concentration of C_{60} NS in LC for constructing the monolayer adsorption in optical cell with 10 mm \times 10 mm (length and width) was roughly calculated to be 0.02 wt% in the case of 10 μm cell gap, the automatic VA layer was achieved on the macroscopic area by homogeneous LC system with 0.1 wt% nanosurfactant. The amount of C_{60} NS was about five times higher than the ideal concentration. To investigate the effect of dissolved C_{60} NS within the LC media, the 0.1 wt% of C_{60} NS-doped optical cell was initially fabricated in the same way as described for the first set of experiments. After checking the formation of VA of molecules, the LC media with excessive amount of C_{60} NS not adsorbed onto the solid substrate was then leached from the cell by immersing in cyclohexane for 3 d. Finally, the optical cell with only C_{60} NS on the top of the surface was prepared. Thereafter, the cell was heated to evaporate the solvent overnight to ensure complete removal of all solvent before refilling the pure LC. As expected, refilling the LC into the C_{60} NS preloaded optical cell also exhibits a perfect VA of LC at room temperature (Figure S16, Supporting Information). There was no discernible agglomeration such as micelles on a micrometer length scale. To confirm the electro-optical responses, the threshold voltage (V_{th}) was determined to be 2.51 V at the 10% maximum of transmittance (Figure S17, Supporting Information). This V_{th} value was almost identical to be compared with the result in Figure 6c. Therefore, we can safely conclude that the electro-optical property has not changed much in practice, even though a significant amount of C_{60} NS is dissolved in the bulk LC medium.

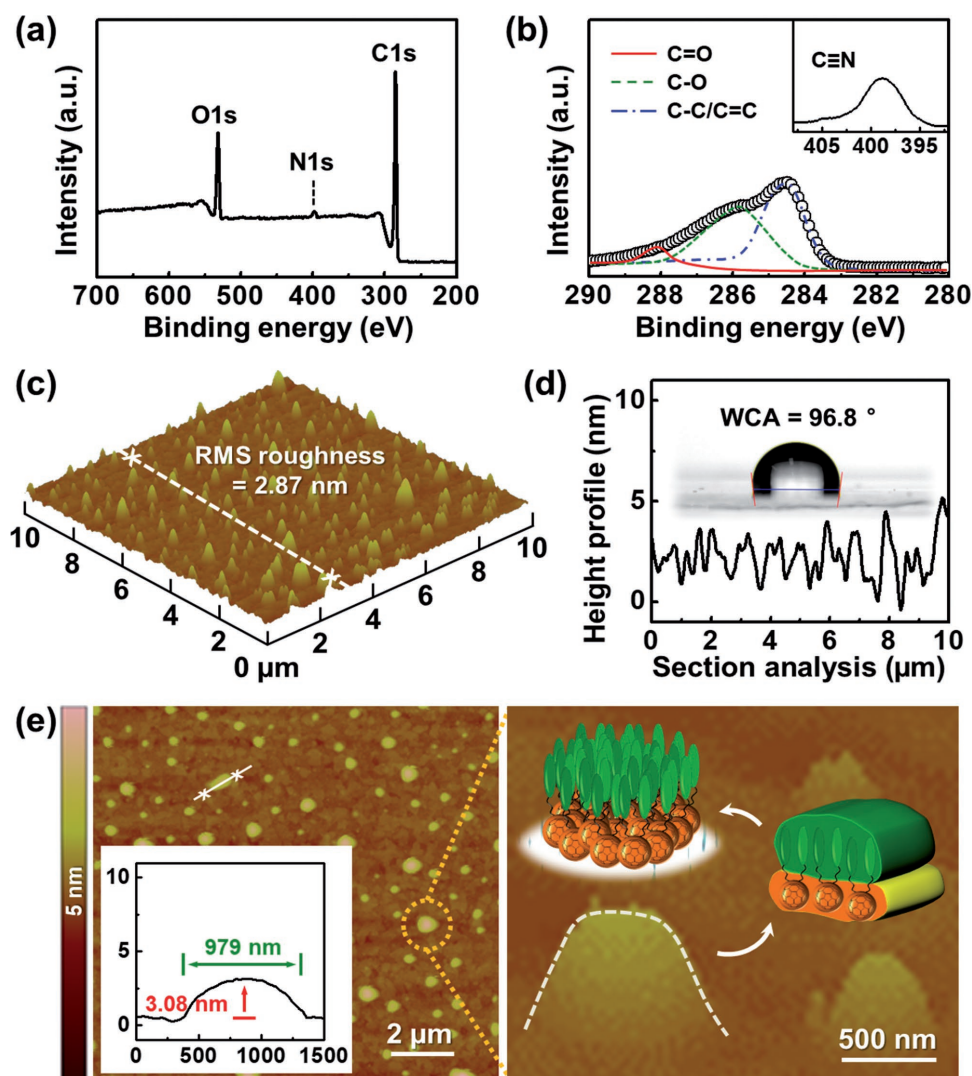


Figure 5. XPS spectra of $C_{60}NS$ deposited film: a) survey scans and b) binding energies of individual peaks. c) AFM image and d) height profile of $C_{60}NS$ monolayer protrusions. e) Topographic analyses of self-assembled $C_{60}NS$ protrusions on the substrate.

The $C_{60}NS$ adsorbed on the inner surface of the substrate originated not only from the strong anchoring interactions between host LC molecules and LC-favoring groups but also from the strong lateral interactions between LC-repelling groups. Thus, the C_{60} groups of $C_{60}NS$ created a nanosized domain on the substrate surface, whereas the tethered cyanobiphenyl mesogens engaged in chemical and physical interactions with host LC molecules. The uniform protrusions of self-assembled $C_{60}NS$ initially induced the homeotropic anchoring of nearby LC molecules, with all LC molecules subsequently standing perpendicular to the substrate surface. To examine the physical interactions between $C_{60}NS$ monolayer and LC molecules, the surface anchoring energy (W) was investigated by the high E field techniques of the optical cell.^[51] From the slope of the graph in Figure 6d, the W is determined to be $8.97 \times 10^{-5} \text{ J m}^{-2}$ by substituting the elastic constant of LC and the cell gap. Note that the W indicates the energetic cost to deviate the LC from its initial orientation.^[52] As a result, the automatically constructed $C_{60}NS$ monolayer over the interface can act as a soft

epitaxial alignment layer by bridging solid substrates and VA of host LC molecules. In addition, the electro-optical responses were reversible when the applied E switching was repeated many times to the multidomain LC cell, clearly indicating that the homeotropic anchoring of LC by $C_{60}NS$ adsorption on the inner surface of the substrate was reasonably strong. Therefore, the ON and OFF switching of birefringence indicated that $C_{60}NS$ nanosurfactant is potentially applicable in LC modulating devices.

3. Conclusion

An asymmetric $C_{60}NS$ nanosurfactant comprising two cyanobiphenyl mesogens and a fullerene nanoatom was successfully synthesized via the Bingel reaction. Systematic experiments revealed that the phase-separation of $C_{60}NS$ from the host LC medium and its subsequent self-assembly on the solid substrates can automatically manipulate the

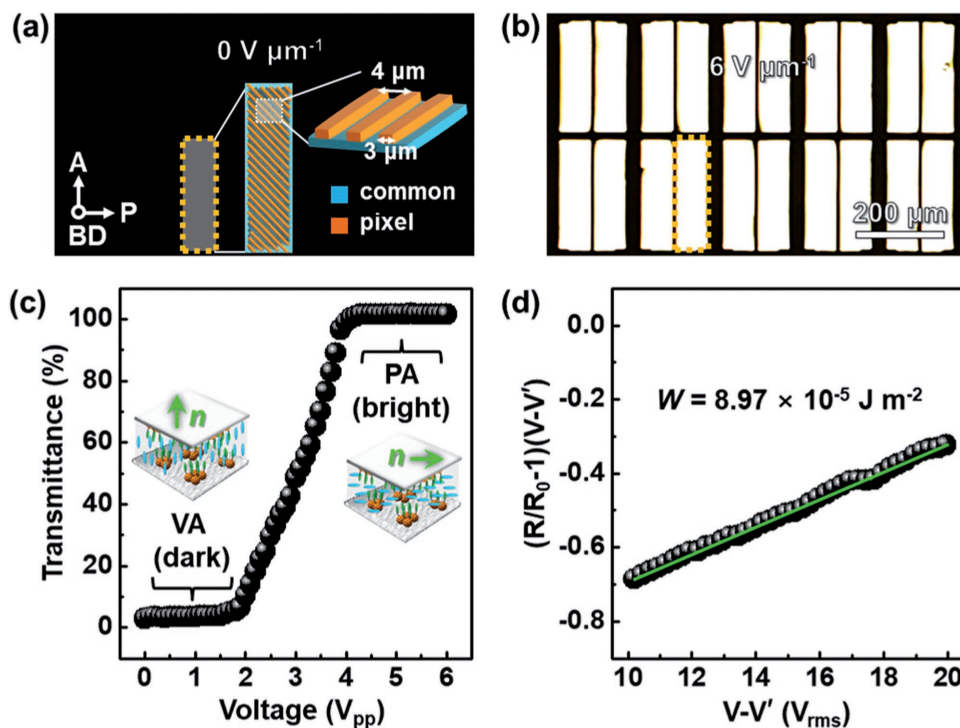


Figure 6. Electro-optical switching behavior of the $C_{60}NS$ -doped multidomain LC cell at voltage a) OFF and b) ON states. c) Voltage dependent-transmittance change and d) surface anchoring energy of the $C_{60}NS$ -doped optical cell.

surface anchoring conditions for the construction of perfect molecular alignment layers on the macroscopic length scale. Scattering and morphological assessment indicated that the self-assembled $C_{60}NS$ monolayer was automatically constructed not only due to the strong anchoring interactions between the host LC molecules and the LC-favoring groups of $C_{60}NS$ but also by virtue of the strong lateral interactions among the LC-repelling groups of $C_{60}NS$. The automatically constructed $C_{60}NS$ alignment layer can be applied in electrically controllable birefringence modulators, being robust and stable toward alternating voltage attacks. Thus, the demonstrated simple but reliable one-bottle approach for the fabrication of automatic molecular alignment of asymmetric nanosurfactant in LC can contribute to the rational design of nanomaterials and predictive capabilities of nanoscale engineering on complex surfaces.

4. Experimental Section

Synthesis: A solution of compound BP_2T (0.15 mmol) and C_{60} (0.35 mmol) in 200 mL of anhydrous toluene was stirred at room temperature under nitrogen atmosphere. After 1 h, 1,8-diazabicyclo[5.4.0]-undec-7-ene (0.35 mmol) and tetrabromomethane (0.15 mmol) were added and stirred at 90 °C for 24 h. The solvent was removed in vacuum. The crude mixture was purified by column chromatography on silica gel using chloroform:methanol = 50:1 to yield $C_{60}NS$ as brown powders (yield: 88%). 1H NMR (400 MHz, $CDCl_3$, δ): 7.74 (d, 4H), 7.65 (d, 4H), 7.58 (d, 4H), 6.93 (d, 4H), 4.63 (t, 4H), 3.99 (t, 4H), 1.88 (m, 4H), 1.75 (m, 4H), 1.64 (m, 4H), 1.31 (m, 4H) ppm; EM calcd (%) for $C_{101}H_{40}N_2O_6$, found: C 88.07, H 2.93, N 2.03; UV-vis ($CHCl_3$, nm):

$\lambda_{max} = 258, 297, 330$; FT IR (KBr, cm^{-1}): $\nu = 2223$ ($C\equiv N$), 1741 ($C=O$), 1108 ($C-O-C$), 526 (C_{60}).

Preparation: The unpatterned and fishbone-patterned ITO glass was washed with distilled water, acetone, and isopropyl alcohol several times, and dried in oven at 80 °C for 1 h. The substrates were assembled by utilizing an automatic press (Neo System). The cell gap was controlled to be 10 μm by applying a spacer. The homogeneous solution of $C_{60}NS$ nanosurfactant and LC mixture were prepared by heating up to 120 °C in the hot plate for 30 min. The certain concentration of $C_{60}NS$ nanosurfactant and LC mixtures were loaded into the optical cell by capillary action.

Measurement: To investigate the surface anchoring energy of $C_{60}NS$ on substrate with LC, $(R/R_0 - 1)(V - V')$ is plotted with respect to $V - V'$, where R and R_0 is phase and maximum retardation, respectively. V' is $\sigma\beta V_{th}$, where $\sigma = (1/\pi) \int_0^1 \sqrt{(1+\beta)(1+km)/(1+\beta)m} dm$, $\beta = (\epsilon_N/\epsilon_P) - 1$, and $k = (K_S/K_B) - 1$. Here, K_S and K_B stand for the splay and bend elastic constants; ϵ_N and ϵ_P mean the components of the dielectric tensors which are normal and parallel to the director, respectively.

Characterization: 1H NMR (JEOL JNM EX400), EM (Vario EL), UV-vis (JASCO ARSN 733), and FT IR spectroscopy (Shimadzu Tracer 100) were employed to identify the chemical structure and purity. The change of optical texture was observed using POM (Nikon E600POL). XRD (Rigaku Imaging System) patterns were obtained by 18 kW rotating anode generator. Simulation software (Cerius² Accelrys) was used to calculate the minimal energy geometry. TEM (Jeol 1230) was utilized with an accelerating voltage of 120 kV to record and the images were taken using a charge coupled device. XPS analysis was performed by K-Alpha (Thermo Scientific). WCA was measured by contact angle analyzer (Phoenix 300). AFM (Agilent 550) images were recorded using silicon cantilevers. The anisotropic polymer network was confirmed by SEM (Carl Zeiss SUPRA). The macroscopic photographs were captured by a digital camera (Canon EOS 5D). The E field was applied utilizing the waveform generator (Tektronix AFG 3022). Electro-optical switching behaviors were determined by LC measurement system (Sesim

Photonics). Photopolymerization was performed by UV light source (Ushio SP9).

Supporting Information

Supporting Information is available from the Wiley Online Library or from the author.

Acknowledgements

This work was mainly supported by BRL (Grant No. 2015042417) and Mid Career Researcher Program (Grant No. 2016R1A2B2011041) of Korea.

Conflict of Interest

The authors declare no conflict of interest.

Keywords

interface engineering, liquid crystals, nanosurfactants, one-bottle approach, self-assembly

Received: July 17, 2017

Revised: August 20, 2017

Published online: November 14, 2017

- [1] C. G. Clark, G. A. Floudas, Y. J. Lee, R. Graf, H. W. Spiess, K. Müllen, *J. Am. Chem. Soc.* **2009**, *131*, 8537.
- [2] D.-Y. Kim, S. Shin, W.-J. Yoon, Y.-J. Choi, J.-K. Hwang, J.-S. Kim, C.-R. Lee, T.-L. Choi, K.-U. Jeong, *Adv. Funct. Mater.* **2017**, *27*, 1606294.
- [3] Y. Zhang, Q. Liu, H. Mundoor, Y. Yuan, I. I. Smalyukh, *ACS Nano* **2015**, *9*, 3097.
- [4] D.-Y. Kim, S.-I. Lim, D. Jung, J.-K. Hwang, N. Kim, K.-U. Jeong, *Liq. Cryst. Rev.* **2017**, *5*, 34.
- [5] T. Kato, Y. Hirai, S. Nakaso, M. Moriyama, *Chem. Soc. Rev.* **2007**, *36*, 1857.
- [6] Y. J. Cha, M.-J. Gim, H. Ahn, T. J. Shin, J. Jeong, D. K. Yoon, *ACS Appl. Mater. Interfaces* **2017**, *9*, 18355.
- [7] A. Sharma, T. Mori, H.-C. Lee, M. Worden, E. Bidwell, T. Hegmann, *ACS Nano* **2014**, *8*, 11966.
- [8] H. Eimura, D. S. Miller, X. Wang, N. L. Abbott, T. Kato, *Chem. Mater.* **2016**, *28*, 1170.
- [9] J. J. Schwartz, A. M. Mendoza, N. Wattanatorn, Y. Zhao, V. T. Nguyen, A. M. Spokoynny, C. A. Mirkin, T. Baše, P. S. Weiss, *J. Am. Chem. Soc.* **2016**, *138*, 5957.
- [10] D. Zhao, W. Zhou, X. Cui, Y. Tian, L. Guo, H. Yang, *Adv. Mater.* **2011**, *23*, 5779.
- [11] J. Hoogboom, P. M. L. Garcia, M. B. J. Otten, J. A. A. W. Elemans, J. Sly, S. V. Lazarenko, T. Rasing, A. E. Rowan, R. J. M. Nolte, *J. Am. Chem. Soc.* **2005**, *127*, 11047.
- [12] W. Zhou, L. Lin, D. Zhao, J. Guo, *J. Am. Chem. Soc.* **2011**, *133*, 8389.
- [13] M. Talarico, B. Carbone, R. Barberi, A. Golemme, *Appl. Phys. Lett.* **2004**, *85*, 528.
- [14] A. Patra, C. G. Chandaluri, T. P. Radhakrishnan, *Nanoscale* **2012**, *4*, 343.
- [15] S. Kundu, M.-H. Lee, S. H. Lee, S.-W. Kang, *Adv. Mater.* **2013**, *25*, 3365.
- [16] H. Qi, T. Hegmann, *ACS Appl. Mater. Interfaces* **2009**, *1*, 1731.
- [17] D.-Y. Kim, S. Kim, S.-A. Lee, Y.-E. Choi, W.-J. Yoon, S.-W. Kuo, C.-H. Hsu, M. Huang, S. H. Lee, K.-U. Jeong, *J. Phys. Chem. C* **2014**, *118*, 6300.
- [18] W. Zhang, Y. Chu, G. Mu, S. A. Eghtesadi, Y. Liu, Z. Zhou, X. Lu, M. A. Kashfpour, R. S. Lillard, K. Yue, T. Liu, S. Z. D. Cheng, *Macromolecules* **2017**, *50*, 5042.
- [19] D. Luo, C. Yan, T. Wang, *Small* **2015**, *11*, 5984.
- [20] A. C. Stelson, S. J. Penterman, C. M. L. Watson, *Small* **2017**, *13*, 1603509.
- [21] D.-Y. Kim, S.-A. Lee, M. Park, Y.-J. Choi, W.-J. Yoon, J. S. Kim, Y.-T. Yu, K.-U. Jeong, *Adv. Funct. Mater.* **2016**, *26*, 4242.
- [22] Y. Li, W.-B. Zhang, I.-F. Hsieh, G. Zhang, Y. Cao, X. Li, C. Wesdemiotis, B. Lotz, H. Xiong, S. Z. D. Cheng, *J. Am. Chem. Soc.* **2011**, *133*, 10712.
- [23] S. Zhang, S. Kumar, *Small* **2008**, *4*, 1270.
- [24] H. Liu, J. Luo, W. Shang, D. Guo, J. Wang, C.-H. Hsu, M. Huang, W. Zhang, B. Lotz, W.-B. Zhang, T. Liu, K. Yue, S. Z. D. Cheng, *ACS Nano* **2016**, *10*, 6585.
- [25] C.-G. Lin, W. Cheng, S. Omwoma, Y.-F. Song, *J. Mater. Chem. C* **2015**, *3*, 15.
- [26] A. M. López, A. Mateo-Alonso, M. Prato, *J. Mater. Chem.* **2011**, *21*, 1305.
- [27] X. Zhang, C.-H. Hsu, X. Ren, Y. Gu, B. Song, H.-J. Sun, S. Yang, E. Chen, Y. Tu, X. Li, X. Yang, Y. Li, X. Zhu, *Angew. Chem., Int. Ed.* **2015**, *54*, 114.
- [28] D.-Y. Kim, M. Park, S.-A. Lee, S. Kim, C.-H. Hsu, N. Kim, S.-W. Kuo, T.-H. Yoon, K.-U. Jeong, *Soft Matter* **2015**, *11*, 58.
- [29] E. Allard, F. Oswald, B. Donnio, D. Guillon, J. L. Delgado, R. Langa, R. Deschenaux, *Org. Lett.* **2005**, *7*, 383.
- [30] D.-Y. Kim, P. Nayek, S. Kim, K. S. Ha, M. H. Jo, C.-H. Hsu, Y. Cao, S. Z. D. Cheng, S. H. Lee, K.-U. Jeong, *Cryst. Growth Des.* **2013**, *13*, 1309.
- [31] X. Zhou, S.-W. Kang, S. Kumar, R. R. Kulkarni, S. Z. D. Cheng, Q. Li, *Chem. Mater.* **2008**, *20*, 3551.
- [32] D.-Y. Kim, C. Nah, S.-W. Kang, S. H. Lee, K. M. Lee, T. J. White, K.-U. Jeong, *ACS Nano* **2016**, *10*, 9570.
- [33] K. M. Lee, T. H. Ware, V. P. Tondiglia, M. K. McBride, X. Zhang, C. N. Bowman, T. J. White, *ACS Appl. Mater. Interfaces* **2016**, *8*, 28040.
- [34] S.-k. Ahn, T. H. Ware, K. M. Lee, V. P. Tondiglia, T. J. White, *Adv. Funct. Mater.* **2016**, *26*, 5819.
- [35] I. Dierking, *Textures of Liquid Crystals*, Wiley-VCH, Weinheim, Germany **2004**.
- [36] D.-Y. Kim, D.-G. Kang, S. Shin, T.-L. Choi, K.-U. Jeong, *Polym. Chem.* **2016**, *7*, 5304.
- [37] N. Kim, D.-Y. Kim, M. Park, Y.-J. Choi, S. Kim, S. H. Lee, K.-U. Jeong, *J. Phys. Chem. C* **2015**, *119*, 766.
- [38] M. Park, W.-J. Yoon, D.-Y. Kim, Y.-J. Choi, J. Koo, S.-I. Lim, D.-G. Kang, C.-H. Hsu, K.-U. Jeong, *Cryst. Growth Des.* **2017**, *17*, 1707.
- [39] D.-Y. Kim, D.-G. Kang, M.-H. Lee, J.-S. Kim, C.-R. Lee, K.-U. Jeong, *Chem. Commun.* **2016**, *52*, 12821.
- [40] D.-Y. Kim, S.-A. Lee, H. Kim, S. M. Kim, N. Kim, K.-U. Jeong, *Chem. Commun.* **2015**, *51*, 11080.
- [41] D.-Y. Kim, S.-A. Lee, D.-G. Kang, M. Park, Y.-J. Choi, K.-U. Jeong, *ACS Appl. Mater. Interfaces* **2015**, *7*, 6195.
- [42] L. Li, M. Salamoneczyk, A. Jáklí, T. Hegmann, *Small* **2016**, *12*, 3944.

- [43] D. Zhao, Y. Peng, L. Xu, W. Zhou, Q. Wang, L. Guo, *ACS Appl. Mater. Interfaces* **2015**, *7*, 23418.
- [44] S.-A Lee, D.-Y. Kim, K.-U. Jeong, S. H. Lee, S. Bae, D.-S. Lee, G. Wang, T.-W. Kim, *Org. Electron.* **2015**, *27*, 18.
- [45] A.-N. Cha, S.-A Lee, S. Bae, S. H. Lee, D. S. Lee, G. Wang, T.-W. Kim, *ACS Appl. Mater. Interfaces* **2017**, *9*, 2730.
- [46] R. K. Roy, E. B. Gowd, S. Ramakrishnan, *Macromolecules* **2012**, *45*, 3063.
- [47] D.-Y. Kim, S.-A Lee, M. Park, K.-U. Jeong, *Chem. - Eur. J.* **2015**, *21*, 545.
- [48] S. H. Lee, S. S. Bhattacharyya, H. S. Jin, K.-U. Jeong, *J. Mater. Chem.* **2012**, *22*, 11893.
- [49] M. Kim, R. K. Mishra, R. Manda, G. Murali, T.-H. Kim, M.-H. Lee, M. Yun, S. Kundu, B.-S. Kim, S. H. Lee, *RSC Adv.* **2017**, *7*, 16650.
- [50] S. Y. Oh, S.-W. Kang, *Opt. Express* **2013**, *21*, 31367.
- [51] W.-J. Yoon, Y.-J. Choi, D.-Y. Kim, J. S. Kim, Y.-T. Yu, H. Lee, J.-H. Lee, K.-U. Jeong, *Macromolecules* **2016**, *49*, 23.
- [52] P. Im, Y.-J. Choi, W.-J. Yoon, D.-G. Kang, M. Park, D.-Y. Kim, C.-R. Lee, S. Yang, J.-H. Lee, K.-U. Jeong, *Sci. Rep.* **2016**, *6*, 36472.